A SYNOPSIS ON

"Design and Synthesis of Some Novel Anti-tubercular Agents"

For submission of Ph.D. thesis

By

Monica Chauhan

Research Guide

Dr. Prashant Murumkar

Pharmacy Department

Faculty of Pharmacy, Kalabhavan Campus,

The Maharaja Sayajirao University of Baroda

Vadodara-390001

1. Introduction

Tuberculosis (TB) is one of the major infectious diseases causing death worldwide. It is a contagious airborne, chronic, granulomatous, and infectious disease, occurring in oropharyngeal region disease which turned out to be fatal if it is not treated properly. TB is usually caused by single infectious agent *mycobacterium tuberculosis* (*Mtb*) mostly affecting lungs along with other parts of the body in some cases. As per the WHO Global tuberculosis report 2020, India is the country with highest burden of tuberculosis [1]. Actually TB is an old disease known as disease of past observed somewhere around seventh and sixth centuries BC [2]. TB got intensified century by century and as years passed, experts all over the world put forth number of findings either to treat TB or adding valuable information about it. During the nineteenth century, in the year 1860, Louis Paster reported TB as airborne transmitted disease whereas Jean Antoine Villemin, a French physician, proved TB as contagious disease in 1865. Thereafter a German physician, Dr. Robert Koch discovered *mycobacterium tuberculosis* (*Mtb*) an infectious agent causing TB in 1882 which was the stepping stone of the program to control and terminate the crisis of this lethal disease [3]. However, despite the identification of causative agent of TB, no any medication was available for the treatment of TB till 1943. In the year 1944, streptomycine was identified to kill *Mtb* and first drug to manage TB. In subsequent years, isoniazide (**1**, INH, 1952), pyrazinamide (**2**, PZA, 1952), ethambutol (**3**, EMB, 1961) and rifampicin (**4**, RIF, 1963) (**Figure1**) were reported to use clinically for the treatment of TB as first-line agents [4]. With this antitubercular regimen for the effective management of TB, it was considered that this old disease was curable and controllable which would be completely diminished in the coming years. But unfortunately, this has not happened and in early 1990s, TB started infecting people again and gaining researcher's attention with the new drug-resistant strains of *Mtb* [5].

First-line Drugs

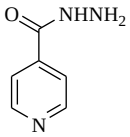

Isoniazide (**1**)

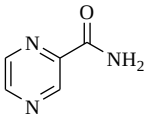

Pyrazinamide (**2**)

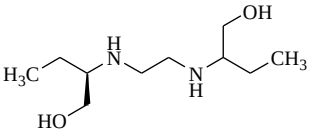

Ethambutol (**3**)

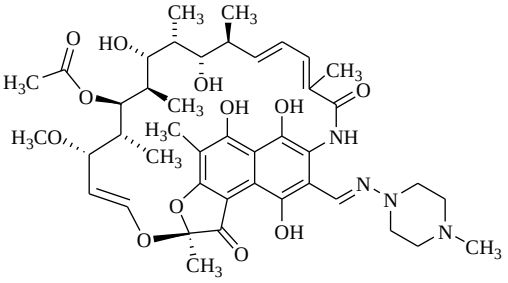

Rifampicin (**4**)

Second-line Drugs

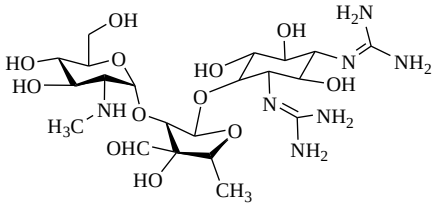

Streptomycin (**5**)

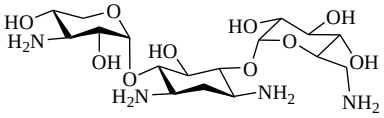

Kanamycin (**6**)

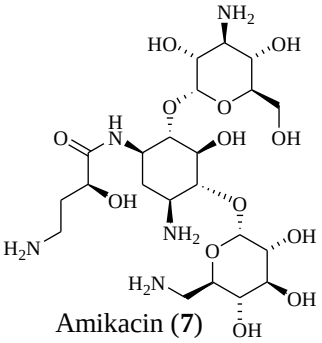

Amikacin (**7**)

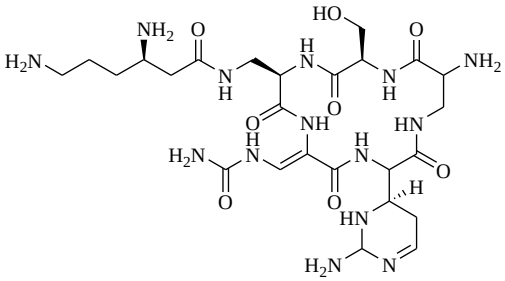

Capreomycin (**8**)

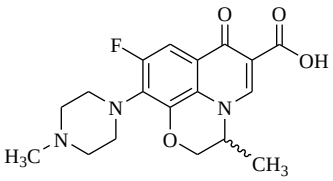

Ofloxacin (**9**)

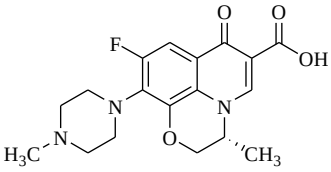

Levofloxacin (**10**)

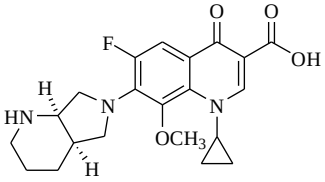

Moxifloxacin (**11**)

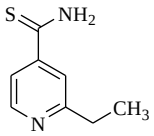

Ethionamide (**12**)

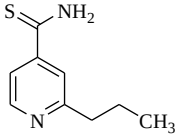

Prothionamide (**13**)

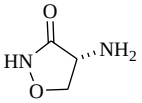

Cycloserin (**14**)

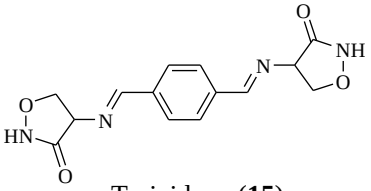

Terizidone (**15**)

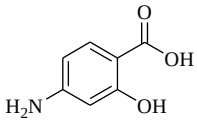

p-Aminosalicylic acid (**16**)

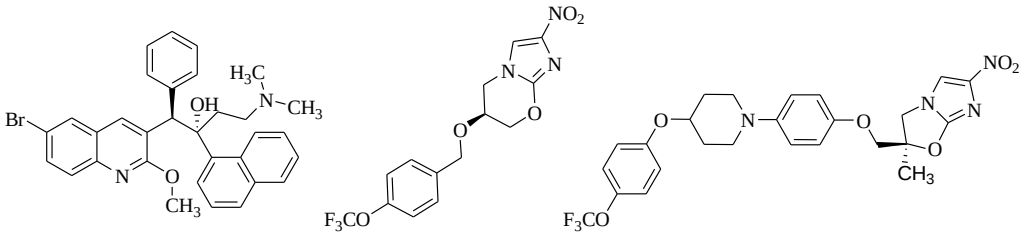

Bedaquiline **(17)** Pretomanid (**18**) Delamanid **(19)**

Figure. 1: Chemical structures of first-line (**1-4**) and second-line (**5-19**) anti-TB drugs.

But this current regimen is associated with issues like efficacy and safety of agents, side effects, toxicity, development of extensive bacterial resistance, Multidrug resistant TB (MDR-TB), Extensively drug resistant TB (XDR-TB) and these issues need to be addressed by new molecules. MDR-TB is defined as resistance to both isoniazid and rifampicin. In India MDR-TB accounts for 2.8% of all new TB cases and 12-17% of retreatment cases. XDR-TB are the cases that are also resistant to fluoroquinolones as well as to the injectable 2nd line drugs [6, 7].

The inadequate armory of drugs in widespread use for the treatment, development of drug-resistant forms of the disease against most commonly used drug isoniazid, and lack of affordable new drugs are the limiting factors in fight against tuberculosis. Hence, there are unmet medical needs for novel, efficacious therapies that minimize resistance problems in *M.* tuberculosis [8].

Drug target identification is the first step of any drug discovery program. Medicinal chemists from all over the world have actively been involved to unravel the novel TB targets with their promising inhibitors. To be an ultimate target for TB drugs, target should possess three essential characteristics which include i) significance for the growth and persistence of bacteria, ii) selectivity (it should be present in the bacteria not in the host) and iii) drug approachability (No structural barriers of bacteria block the approach of drug to target). It could be possible to identify novel TB targets simply by screening a library of therapeutics over *Mtb* growth *in vitro* followed by identification of their targets. But it doesn't appear as simple as stated because it is merely possible to attain it. Numerous Anti-TB drugs have already been used clinically to treat TB but the real fact is that the exact target has not been recognized yet for many of them [9]. There are several targets identified till date for the inhibition of all active, replicating and dormant forms of TB.

The cell wall rich in lipids such as mycolic acid makes the treatment of TB difficult. The peculiar ability of Mtb to modify its metabolism in such a way to slow down replication, therefore surviving in a dormant state (NRP-TB, non-replicating persistent TB) and withstanding the therapy, is the cause of the long-lasting period of treatment [10].

It is needed that novel antitubercular agents, either individual or in combination, should have shorter duration of treatment and manage MDR- and XDR-TB effectively with minimum or lower toxicities. Recently, decaprenyl-phosphoribose 2′-epimerase (DprE1) enzyme possessing all these requirements has been promptly emerged as a potential novel drug target for TB drug discovery [11]. DprE1 is a flavo-enzyme present in the periplasmic space of mycobacterial cell wall which is essential for the mycobacterial cell wall metabolism[12]. Significance of DprE1 as a new druggable target for the discovery of antitubercular drugs would be thoroughly discussed in the following section of this chapter.

2. Decaprenylphosphoryl-β-D-ribose 2'-epimerase (DprE1): a viable target for development of anti-TB agents.

Considering its function to provide overall strength to the cell and protect the cell from virulence and pathogenicity cell wall is the most important component of a bacterial cell [13]. Therefore, cell wall biosynthesis has been considered as the most promising target for most of the drugs including some antibiotics. Biosynthesis of cell wall in *Mtb* consists of a of number of processes which in turn have been found to be ideal drug targets for the discovery of anti-TB drugs [14]. Several anti-TB agents such as isoniazid (**1**) and ethambutol (**3**) of first-line category along with other second-line agents actually interfere in the biosynthesis of the cell wall in different stages [15, 16].

Composition of the *Mtb* cell wall is quite complex as it is made up of two unique complexes known as peptidoglycan-arabinogalactan-mycolic acid (PAM) complex or mAGP complex (mycolyl-arabinogalactan–peptidoglycan) and lipoarabinomannan (LAM) [17]. PAM complex is mainly composed of three layers, a) a highly impermeable lining of mycolic acid, b) arabinogalactan polysachharide (AG) and c) peptidoglycan (PG), posing from outer side to inner side of the cell. Peptidoglycan (PG) is covalently bound to arabinogalactan (AG) through a phosphodiester linkage which further gets attached to mycolic acid forming PAM complex [18]. The second component of the *Mtb* cell wall i.e. lipoarabinomannan is a non-covalently bound

lipopolysaccharide comprising of *D*-arabinofuranose (Araf) and mannopyranosyl residues. Both the components (PAM and LAM) are a prerequisite to maintain the cell wall integrity and impart a crucial role in the *Mtb* virulence and pathogenesis [16, 19, 20].

Synthesis of Araf residues, essential building blocks of AG and LAM, is a crucial biosynthetic step. Biosynthesis of AG and LAM involves the addition of Araf residues to the galactan and mannan domains respectively, catalyzed by a specific enzyme known as arabinosyltransferase. The arabinosyltransferase enzyme uses the sugar decaprenylphosphoryl-β-*D*-arabinose (DPA) generated by epimerization of decaprenylphosphoryl-β-*D*-ribose (DPR). DPA is the only source for the Araf residues in *Mtb*. Without DPA, it is difficult for the bacteria to survive, both the latent and the virulent *Mtb* forms as the whole biosynthesis of *Mtb* cell wall would be stopped [16, 19, 20].

A heterodimeric enzyme i.e. decaprenylphosphoryl-β-*D*-ribose 2'-epimerase (DprE) consisting of two enzymes DprE1 and DprE2, the key proteins is responsible for the biosynthesis of DPA. Decaprenylphosphoryl-β-*D*-ribofuranose 2-oxidase (DprE1) is an FAD-dependent enzyme that converts DPR to decaprenylphosphoryl-2-keto-β-*D-erythro*-pentofuranose (DPX) by oxidation, and DPX is then further reduced to DPA in presence of decaprenylphosphoryl-*D*-2-keto-*erythro*-pentose reductase (DprE2) (**figure 2)**. DprE1 is an important enzyme required for the growth and survival of *Mtb*. Hence, blockade of DPA synthesis by inhibition of DprE1 enzyme would be a key strategy to stop the biosynthesis of *Mtb* cell wall [12, 21].

DprE1 has evolved as a new competent target which could be exploited for anti-TB drug discovery to tackle the problem of resistance. It was postulated a few decades ago that blocking the biosynthetic process of mycobacterial cell wall would be the best way to win the battle against TB. DprE1 plays a crucial role in the biosynthesis of *Mtb* cell wall. In fact, inhibition of DprE1 causes cessation of generation of DPA required for the formation of Araf residues. Reduced levels of Araf residues hamper the supply of these essential building blocks of mycobacterial cell wall i.e. AG and LAM, which subsequently affect the biosynthesis of *Mtb* cell wall. Thus, it clearly demonstrates that inhibiting DprE1 could be critical for the growth and survival of *Mtb*. Moreover, DprE1 is an ideal target as it is present only in mycobacteria and not in humans, which certainly underlines its importance as an anti-TB drug target for design, development and discovery of novel anti-TB drugs. These special features of DprE1 enzyme

significantly make it a valuable drug target that could be utilized effectively for the discovery of novel anti-TB agents with enhanced biological potential with minimum toxicity [1, 5, 8].

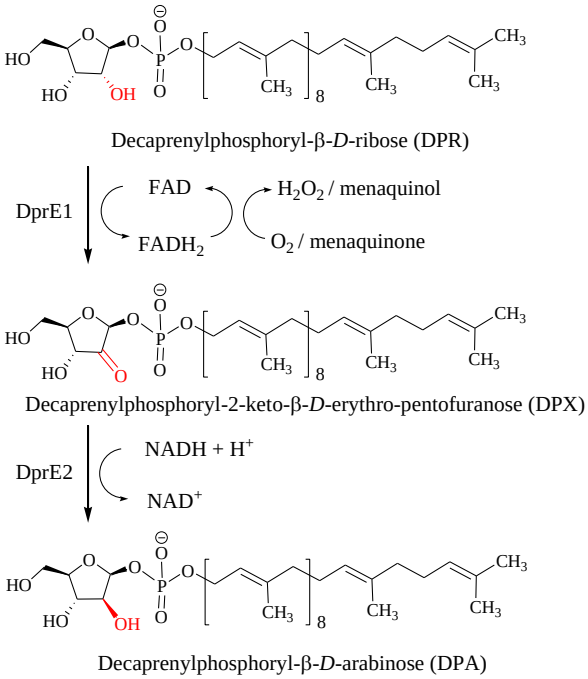

Figure 2: Epimerization of 2′-OH group (highlighted in red color) of DPR by DprE1 and DprE2 to generate DPA in the presence of cofactor FAD and NADH. The reaction takes place in the presence of free oxygen or menaquinone.

The first crystal structure of DprE1 enzyme was disclosed in the year 2012 by Neres*et al.* [22] and Batt*et al.* [23]. Thereafter, approximately 35 crystal structures of DprE1 have been reported till date, which are available in protein data bank.

Crystal structure of DprE1 contains several active sites for the binding of inhibitors. The enzyme DprE1 (PDB code 4P8L, **Figure 3**) consists of two active binding domains, similar to two-domain topology of vanillyl alcohol oxidase family of oxidoreductases. These two active binding domains include an FAD binding domain with residues 7–196, 413–461 and a substrate binding domain with residues 197-412 (**Figure 3**). The two disordered loops actually keep the substrate binding domain wide open facilitating accommodation of the substrate in the domain. Thus, these loops could be considered as the entrance gate for the substrate approaching the substrate binding domain [20].

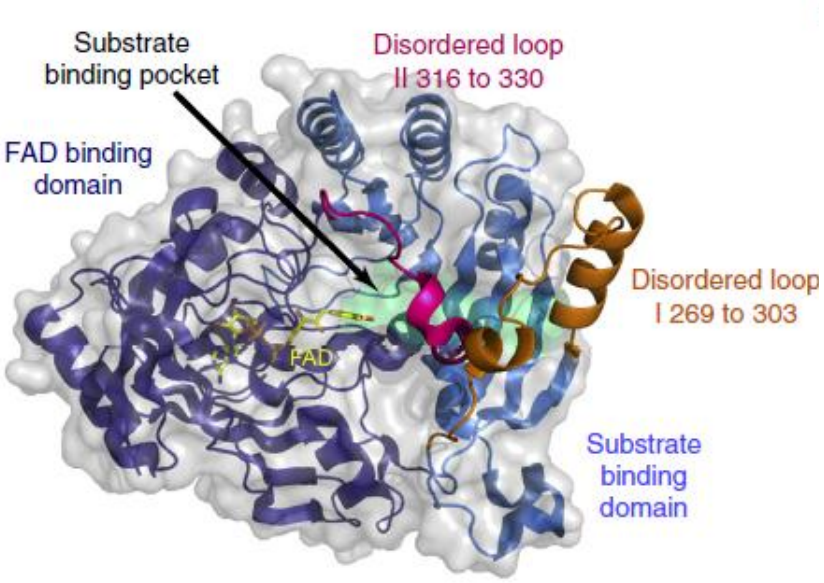

Figure 3: Overall structure of DprE1 (PDB code 4P8L). FAD-binding domain is in deep blue and substrate-binding domain in light blue. Substrate-binding pocket is represented as a lime green surface. The two disordered loops are represented in orange for loop I (residues from 269 to 303) and hot pink for loop II (316 to 330) [7].

3. Literature survey

Numerous researchers throughout the world have been working continuously for the development of novel lead molecules active against M. tuberculosis and can be used in treatment and management of MDR-TB and XDR-TB. Currently, use of molecular hybridization approach is most preferred by scientist for the development of novel lead compounds. Hybrid compounds can be designed by linking pharmacophore subunits directly or with spacers.

Over the decade, many DprE1 inhibitors are reported. Various scaffolds have emerged as DprE1 inhibitors as shown in **figure 4**. Four DprE1 inhibitors namely BTZ-043, Macozinone, OPC-167832 and TBA-7371 are in clinical trials [24].

Thus, this study aims towards the design and synthesis of newer unknown classes of anti-tuberculosis agents. It was planned to gain knowledge of minimum structural requirements required for DprE1 inhibition.

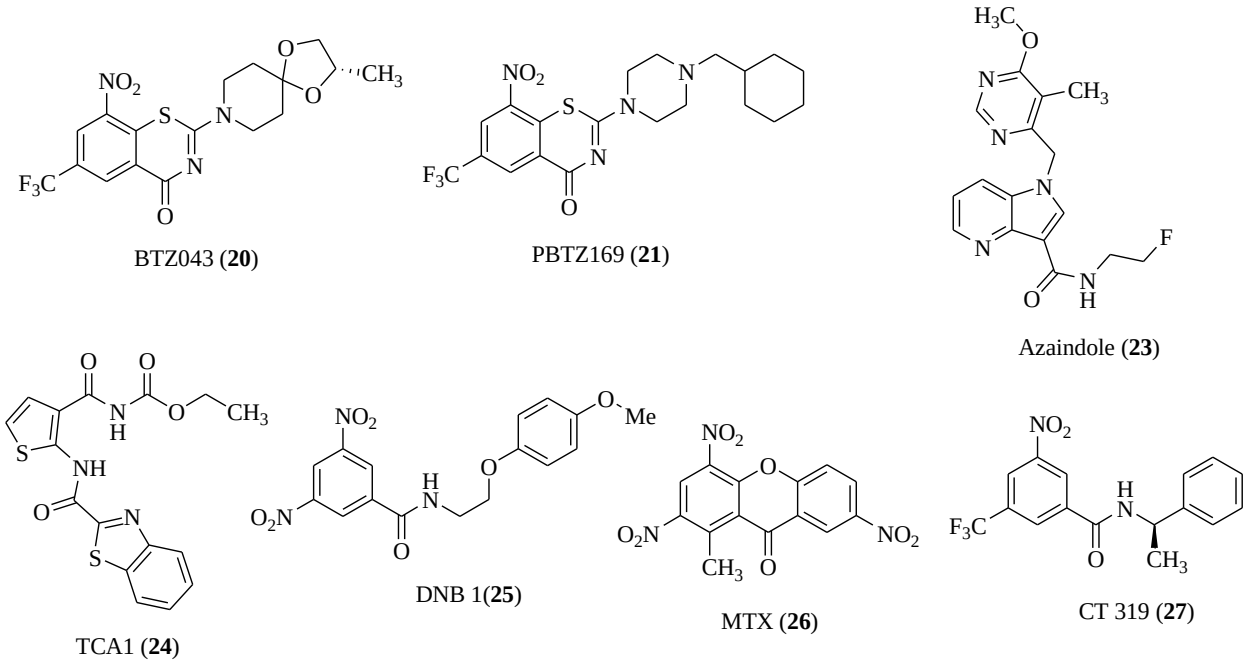

Figure 4: Reported Scaffolds as DprE1 inhibitors

4. AIM AND OBJECTIVES

- The objective of this work is to develop novel derivatives using structure-based design approach like pharmacophore development with specificity for the DprE1 enzyme as target.
- To establish the mechanism of action for inhibitory activity of new molecules through molecular docking, molecular dynamics etc.
- To synthesize the designed compounds and to establish their structures.
- To carry out the *in vitro* and in vivo studies.
- To carry out Quantitative Structure Activity Relationship (QSAR) studies to establish structure activity relationship and to design novel potent molecules in the series.

5. RESULTS AND DISCUSSION

To rationally design novel DprE1 inhibitors, it was aimed to develop pharmacophore model for reported DprE1 inhibitors. This pharmacophore model was then used as primary filter in the virtual screening. The hits obtained after virtual screening were processed and optimized to design the compounds. The detailed procedure used is narrated here.

5.1 Selection of data-set

Many scaffolds have been reported in recent years showing DprE1 inhibition. After conducting thorough literature survey, it was found that 566 compounds from various classes such as benzothiazinones, azaindoles, aminoquinolones, Quinoxalines, triazoles etc were reported as DprE1 inhibitors. Out of these 566 compounds, 300 compounds were selected for which, activity was defined in terms of IC_{50} value. Finally a set of 140 compounds with IC_{50} value ranging from 100 to 0.003 μM were selected in such a way that the data set provide both structural and biological variations. IC_{50} value of these compounds were converted to pIC_{50} values.

Ten compounds were kept aside to be used as external data set for the validation of the model. These 140 compounds were divided into a two sets i.e. training (112) and test set (28) by following the rule (a) both training and test set compounds contain representative from each class to ensure structural diversity; (b) both, training and test sets covered the bioactivities (IC_{50}) as wide as possible. If there was only one compound with maximum order of biological activity in a class, such a compound was assigned to the training set.

5.2 Pharmacophore model generation

The development of pharmacophore model was done using PHASE, version 2.5 (SchrÖdinger). Following steps were carried out to obtain suitable pharmacophore:

- Structures were imported to the "develop pharmacophore model" and minimized by using two-step process i.e. cleaning (geometric refining) using Ligprep module. Conformations were generated by using ConfGen search method with OPLS-2005 force field. A maximum of 1000 conformers per structure with 100 conformers per rotatable bond were generated by a pre-process of 50 steps and a distance-dependent dielectric solvation was applied. Activity threshold was kept as. Active above: 6.9 and inactive below: 5.0.
- A set of pharmacophore features for selected compounds were produced using create sites option. Site points were created for each conformer of the compounds under study. For creating pharmacophore sites, a default setting having Aromatic ring (R), hydrophobic (H), negative (N), positive (P), H-bond donor (D), and acceptor (A) features were used.

- Common pharmacophore hypothesis for the set of active ligands were generated using these features. A set of variants formed by a set of features was used to identify the common pharmacophore using a tree based partitioning algorithm with a criterion that the selected must match maximum number of compounds.
- The generated common pharmacophore of all variants were scored active and inactive compounds to identify a set of hypothesis having best alignment for most of the compounds. The common hypothesis so formed were scored by setting the root mean square deviation (RMSD) value below 1.2 and vector score value to 0.5.
- The most appropriate hypothesis was selected for further exploration. All the generated pharmacophore hypothesis were ranked on the basis of various parameters such as survival score and survival minus 'inactive'. Higher survival score indicates better mapping of the pharmacophore with the active ligands and the fitness score confirms the quality of the pharmacophore that can be defined as how well the compounds could be mapped to a pharmacophore model.

Based on 41 active ligands in the data-set, several 3-point and 4-point pharmacophore hypothesis were generated. These alignments were further used to develop 3D-QSAR model.

5.3 Results of pharmacophore modeling

It was aimed to identify essential structural features for DprE1 inhibitors. Active and inactive threshold were fixed to 6.9 and 5.0 respectively and applied to the data-set, giving 41 active,15 inactive and 84 moderately active compounds. All 41 active compounds were used. The software was restricted to find a minimum of 3 and maximum of 5 sites. Several 3-point and 4-point hypothesis were generated. AHRR, AAR, AAH, ARR, HRR and AHR were found to be most probable hypothesis. All the generated hypothesis were evaluated. Highest ranked survival score for 3-point hypothesis was obtained for AAR.3 i.e. 3.310 whereas 4-point hypothesis AHRR.28 and AHRR.29 were scored as 2.990 and 2.714 respectively. But, hypothesis AHRR showed better results in QSAR and validation. The AHRR.28 containing one hydrogen bond acceptor, one hydrophobic group and two aromatic rings is shown in **figure 5**.

Table 1: Data of the top ranked pharmacophore models.

ID	Survival	Survival inactive	Post hoc score	Site	Vector	selectivity	Match	Energy
AHRR.28	2.990	1.641	2.991	0.63	0.897	1.359	22	2.254
AHRR.29	2.714	1.782	2.714	0.51	0.850	1.362	22	1.185
AAR.4	3.310	2.432	3.310	0.76	0.901	0.848	21	0.467
ARR.3	3.185	1.858	3.185	0.74	0.902	0.897	31	5.843
HRR.30	3.218	2.748	3.218	0.70	0.963	1.069	27	4.784
AHR.47	3.189	2.322	3.189	0.79	0.886	0.979	26	2.034

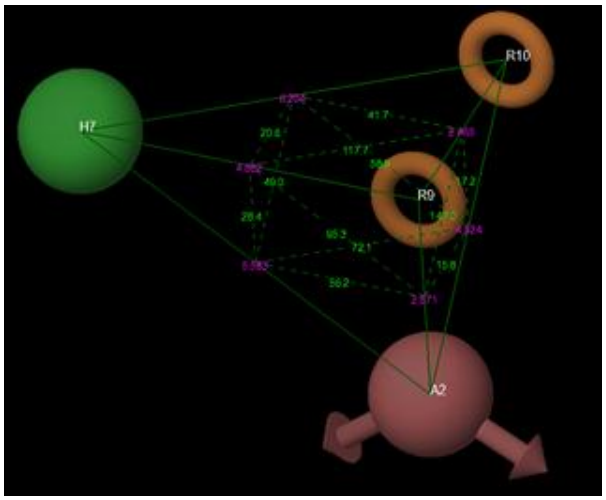

Site 1	Site 2	Distance Å)
A2	H7	5.583
A2	R9	2.671
A2	R10	4.924
H7	R9	4.662
H7	R10	6.204
R9	R10	2.465

Figure 5: Pharmacophore model AHRR.28. Orange colored torus represents aromatic rings (R9 and R10), green colored sphere represents hydrophobic group (H7), and light magenta colored vector represents hydrogen bond acceptor (A2). Purple color represents distances and green color represents the angles between the pharmacophoric features.

Table 2: Angles between the different pharmacophoric features of AHRR.28 model.

Site 1	Site 2	Site 3	Angle
H7	A2	R9	56.2
H7	A2	R10	72.1
R9	A2	R10	15.8
A2	H7	R9	28.4
A2	H7	R10	49.0
R9	H7	R10	20.6
A2	R9	H7	95.3
A2	R9	R10	147.0
H7	R9	R10	117.7
A2	R10	H7	58.9
A2	R10	R9	17.2
H7	R10	R9	41.7

5.4 Development of QSAR model

The developed pharmacophore model was utilized for development of QSAR model. Dataset was divided randomly into training (118 compound) and test set (28 compounds) in such a way that the compounds are divided into 4:1 ratio to give variation in biological activity and structural diversity. A number of models were generated but top ranked model were considered. QSAR model obtained by 4-point hypothesis (AHHR.28) was found to be best model. Statistical parameters of QSAR model are shown in the table.

Table 3: Statistical parameter obtained for the QSAR model obtained from various alignments.

Statistical parameters	AHHR.29	AHRR.28	AHRR.17
R^2	0.8871	0.8520	0.8950
Q^2	0.5950	0.866	0.6133
PLS factor	5	5	5
Stability	0.441	0.172	0.257
F-value	133.5	109.7	148.9
RMSE	0.6844	0.3491	0.6923
SD	0.4075	0.477	0.390
Pearson-R	0.7846	0.9308	0.8061

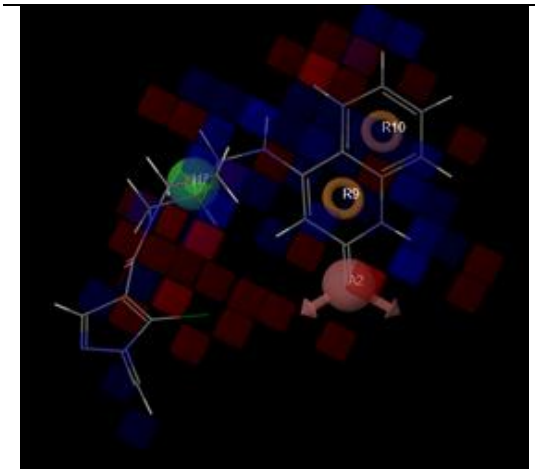

Figure 6: QSAR model visualization (dark blue region showing positive coefficient and red region showing negative coefficient)

5.5 Validation of the pharmacophore model

Pharmacophore model (AHRR.28) was validated using an external set of ten compounds (**Figure 7**) which were not included in the pharmacophore model development. The external set

was chosen in such a way that it included five active compounds (pIC_{50}>6) as well as five inactive

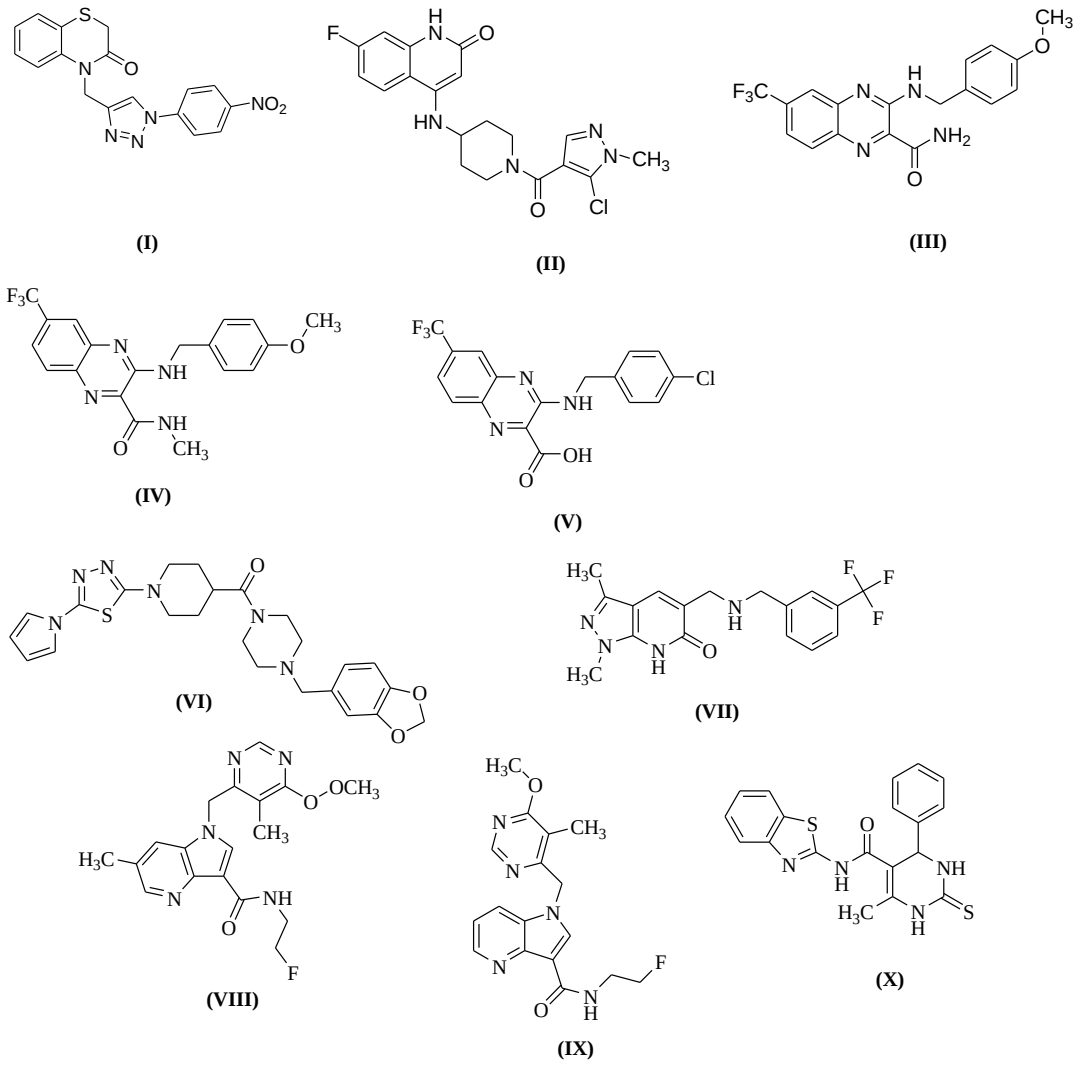

Figure 7: Compounds used for the validation of pharmacophore model (AHRR.28).

compounds (pIC_{50}<6). These compounds were minimized using the same protocol used for the compounds for model generation. Minimized structures were then matched to the hypothesis in "**search for matches**" panel. Four compounds were picked out of ten compounds. It was worth mentioning that out of the five active compounds, four were picked and none of the inactive compounds were picked (**Table 4**). This proves applicability of the developed model.

Table 4: Validation results of ten compounds

Structure	Observed activity (pIC_{50})	Active/inactive	Picked or Not
I	4.183	Inactive	Not
II	8.154	Active	**Picked**
III	4	Inactive	Not
IV	4	Inactive	Not
V	7.3	Active	Not
VI	6.39	Active	**Picked**
VII	4	Inactive	Not
VIII	8.522	Active	**Picked**
IX	8.00	Active	**Picked**
X	5.11	Inactive	Not

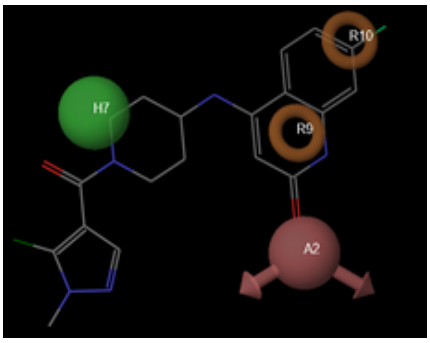

Mapping of II

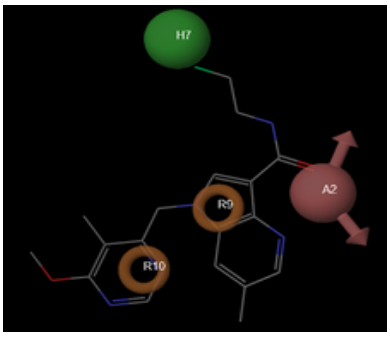

Mapping of IV

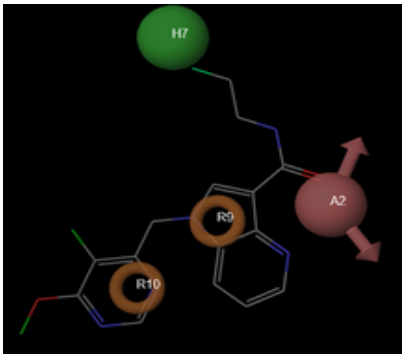

Mapping of VIII

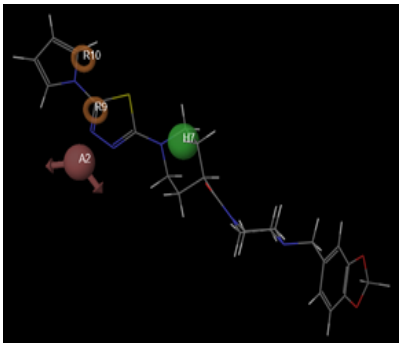

Mapping of IX

Figure 8: Mapping of active structures (**picked**) on pharmacophore model.

5.6 Virtual screening

Virtual screening was carried out with an aim to find potential hits suitable for optimization as DprE1 inhibitors. Asinex database consisting of 2,12,526 chemical compounds with known 3D structures were downloaded and optimized using OPLS 2005 force field in Maestro. Various filters were used (**Figure 9**) to screen out the possibly active compounds. The developed 4-feature pharmacophore model (AHRR.28) was used as the first filter to retrieve structures that fit the pharmacophore hypothesis. The retrieved compounds were further screened using molecular docking studies using Glide. Compounds retrieved from first stage were docked by using High Throughput Virtual screening (HTVS) method and flexible docking mode in Glide. Compounds so obtained were re-docked using standard precision method for getting higher precision. The same process is repeated using extra precision (XP) method. The resulting compounds were further screened for checking the druggablity by using third filter i.e. Lipinski's Rule of five, in which compounds violating one/more than one parameter were not considered for further processing, using QikProp in Maestro. After applying these screens, total 8 hits (H1-H8) were obtained (**Figure 10**).

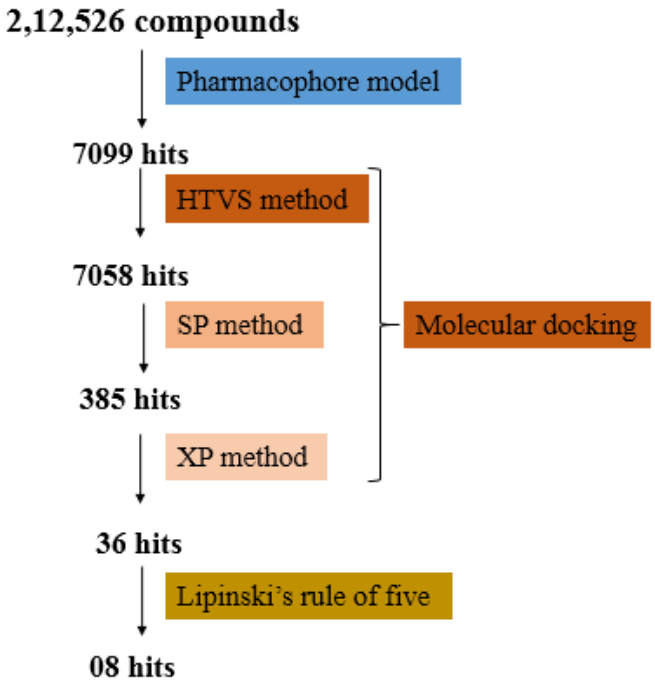

Figure 9: Flow chart of virtual screening

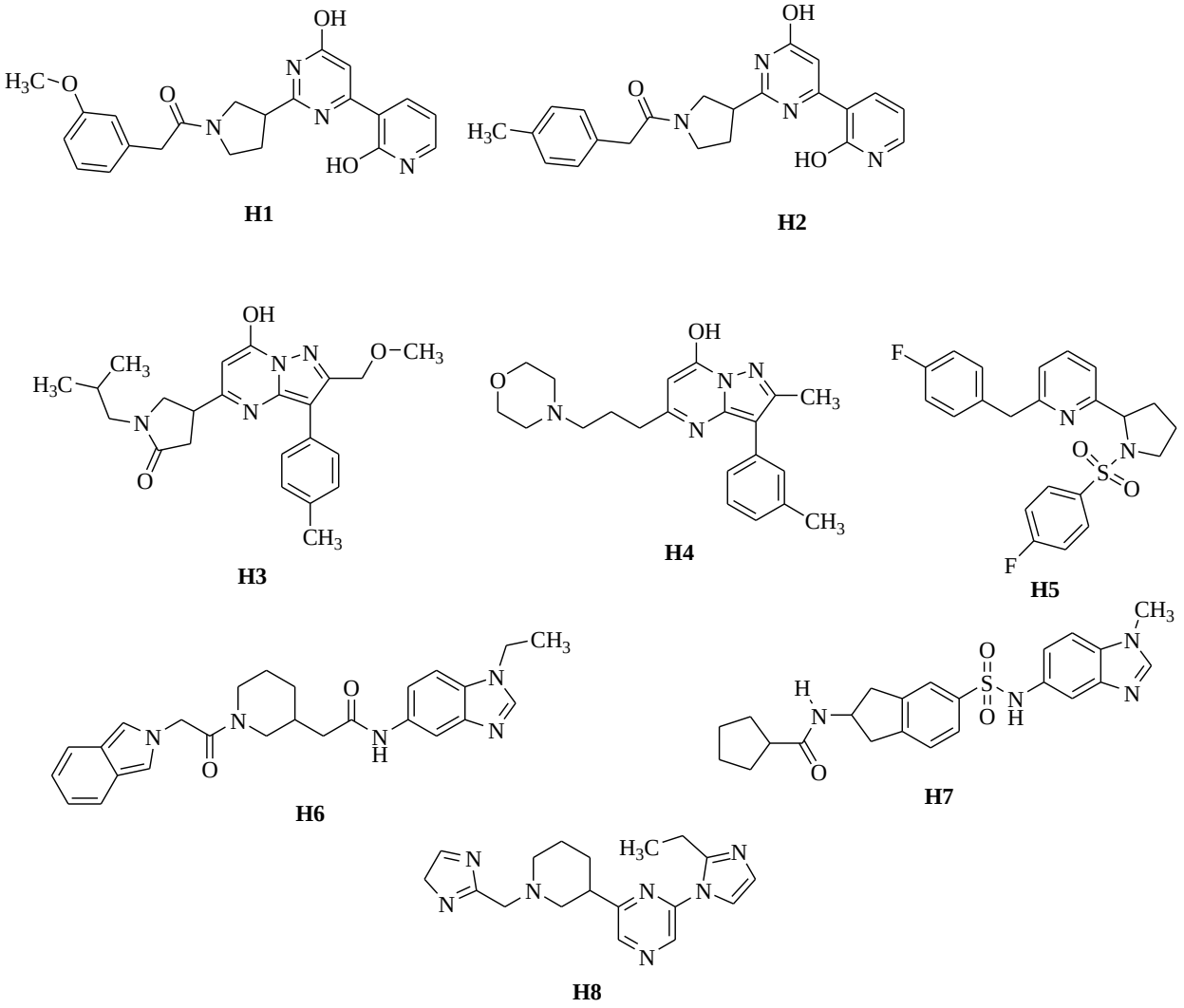

Figure 10: Hits obtained as a out put of virtual screening protocol.

Out of the eight hits obtained from virtual screening, two were pyrazolo-pyrimidine derivatives (H3-H4). This (pyrazolo-pyrimidine) moiety is not yet reported as DprE1 inhibitor. Considering the synthetic feasibility of pyrazolo-pyrimidine moiety, it was selected for further optimization to obtain target compounds. The resultant structures (X**I**, X**II and X III**).

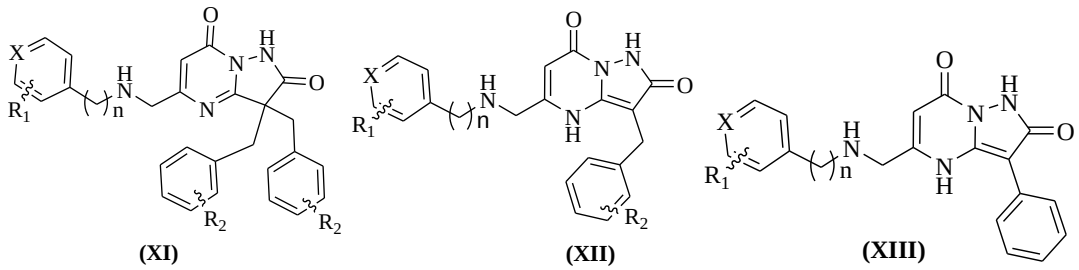

X= N or C; n= 0 or 1

R_1= H, 4-F, 4-Cl, 4-Me, 3,5-di-Cl, 4-OCH_3, 3,4-di-OCH_3

R_2= H, CH_3 and Cl

are further taken up for the synthesis. Structure X**I** represents the bi-substituted series whereas X**II** represents mono-substituted series. We performed ligand-enzyme interaction studies for the di-substituted compound (X**I**) (**Figure 11 and 12**). It was found out that bi-substituted compounds were giving interactions similar to the standard (PDB id: 4p8n, Co-crstal-QN-118).
It was observed that compound **28** was interacting with Ser59 amino acid residue via H-bonding. The compound also showed pi-pi bonding with Tyr60 and His132. It was also showing hydrophobic interactions with Pro116, Val121, Cys129 and Ile131. Halogen at –R was found to be interacting Ala53 amino acid residue.

So, we planned to synthesize both bi-substituted compounds (X**I**) and mono-substituted (X**II**) and the synthetic scheme was optimised accordingly.

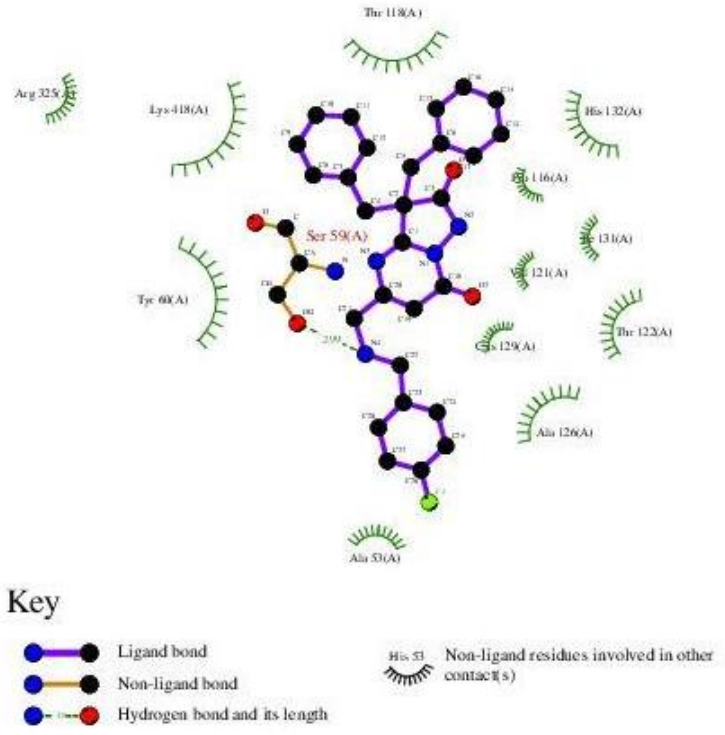

Figure 11: 2-D interactions of compound **28** with DprE1 (PDB id: 4p8n)

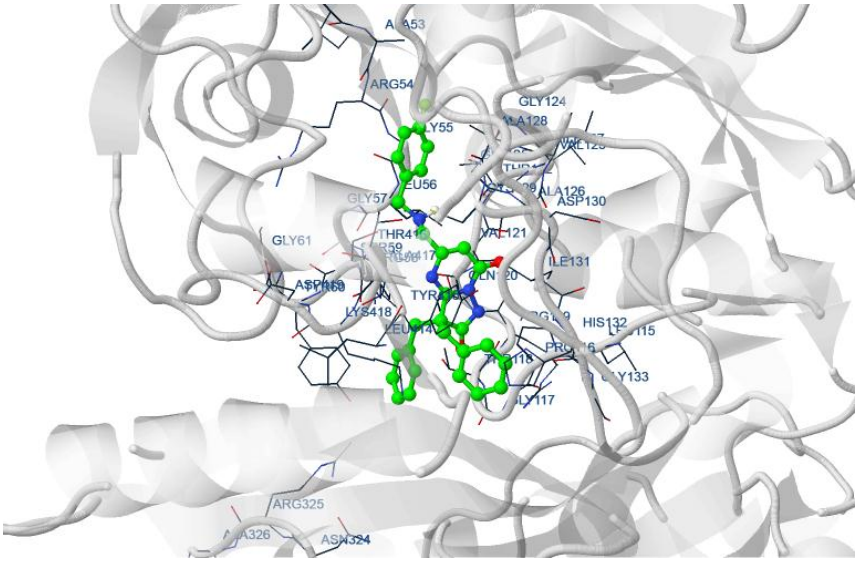

Figure 12: 3-D interactions of compound **28** with DprE1 enzyme. (PDB id: 4p8n)

Scheme for the synthesis of bi-substituted (XI) prototype using scheme

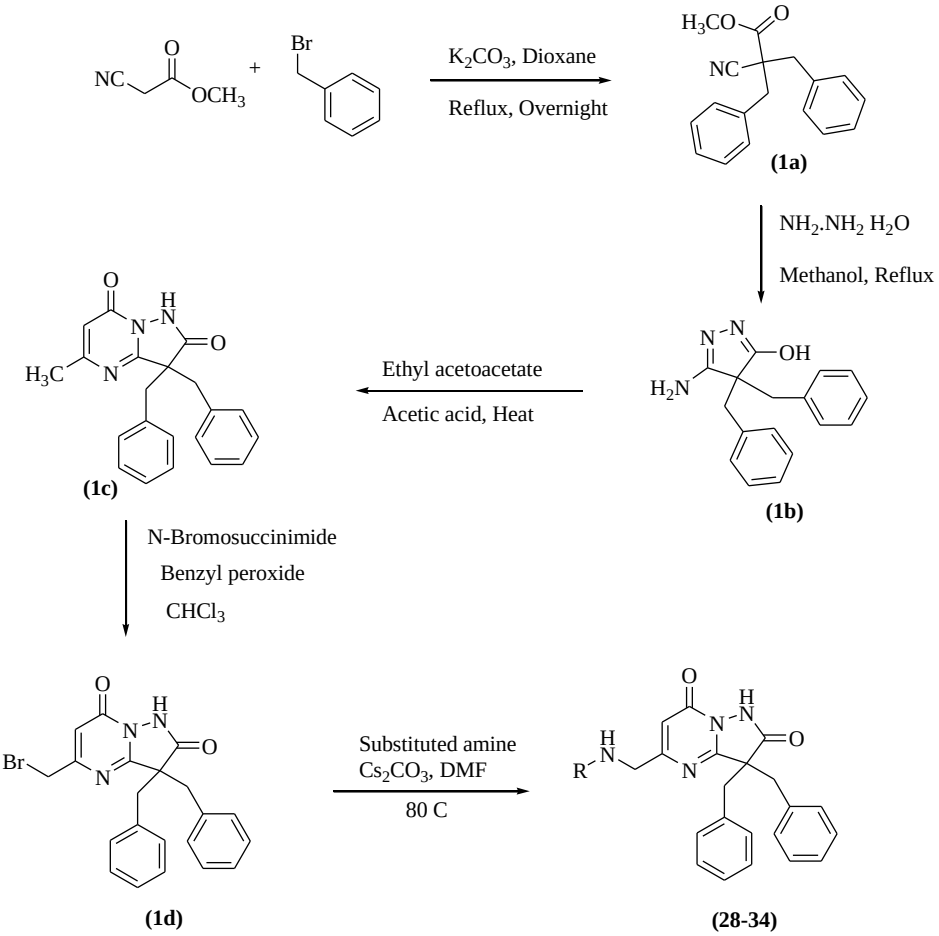

Scheme 1: Synthetic scheme of bi-substituted derivatives (XI)

6. Experimental work done

6.1 Synthesis and characterization of bibenzyl-substituted derivatives

6.1.1 Synthesis of methyl- 2-benzyl-2-cyano-3-phenylpropanoate (1a).

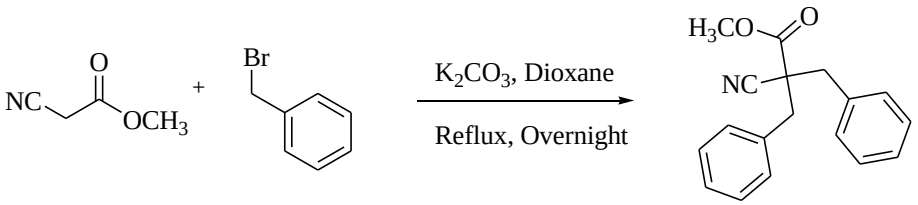

(1a)

To a solution of methyl cyanoacetate and potassium carbonate in dioxane stirred under nitrogen atmosphere at 0° C was added a solution of benzyl bromide in dioxane. The reaction mixture was stirred at 80 °C for overnight. The reaction mixture was diluted with ice cold water and triethylamine and extracted with ethyl acetate (thrice). The combined organic layer was washed with water and brine, dried over anhydrous sodium sulphate and concentrated to dryness in vacuum to obtain buff coloured solid product. This product was directly taken for next step without further purification. Its melting point was observed to be 82-87 °C. **IR** (KBr cm^{-1}): 2965, 2937, 2264, 1743, 1442, 1011 and 846.

6.1.2: Synthesis of 4,4-dibenzyl-5-iminopyrazolidin-3-one (1b)

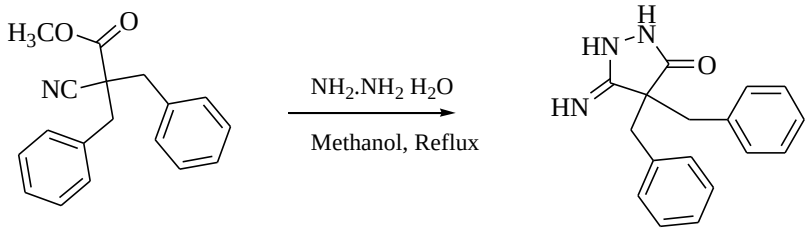

(1b)

To a solution of methyl 2-benzyl-2-cyano-3-phenylpropanoate in methanol stirred under nitrogen environment at room temperature, hydrazine hydrate (99 %) was added drop wise. The reaction mixture was refluxed at 80 °C overnight. After cooling, the reaction mixture was evaporated to dryness in vacuum. The residue was recrystallized using chloroform to provide white coloured solid of 4,4-dibenzyl-5-iminopyrazolidin-3-one having a melting point of 237-239 °C. **IR** (KBr,

cm^{-1}): 3434, 3061, 2923, 2855, 1686, 1632 and 1448. **Mass**: [M -1] - 280.6.**^{1}H-NMR**: δ 9.39 (s, 1H), 7.20-7.14 (m, 10H), 6.183 (s, 1H) and 3.074-2.908 (dd, 4H).

6.1.3: Synthesis of 3,3-dibenzyl-5-methylpyrazolo[1,5-*a*]pyrimidine-2,7(1*H*,3*H*)-dione (1c).

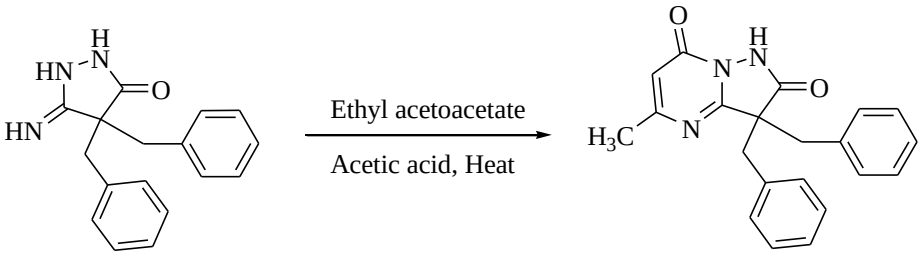

(1c)

To a solution of 4,4-dibenzyl-5-iminopyrazolidin-3-one in acetic acid, ethyl acetoacetate was added drop wise and stirred at room temperature for 10 minutes. Then, the reaction mixture was heated at 100 °C overnight. The reaction mixture was then diluted with ice cold water to obtain white coloured solid product. **Melting Point :** 188-190 °C**. IR** (KBr, cm^{-1}): 3030, 2970, 2925, 2744, 1739, 1683, 1602, 1549, 1393 and 1265. **Mass**: [M+1]- 346.5, [M+2]- 347.6.

6.1.4: Synthesis of 3, 3-dibenzyl-5-(bromomethyl)pyrazolo[1,5-*a*]pyrimidine-2,7(1*H*,3*H*)-dione (1d).

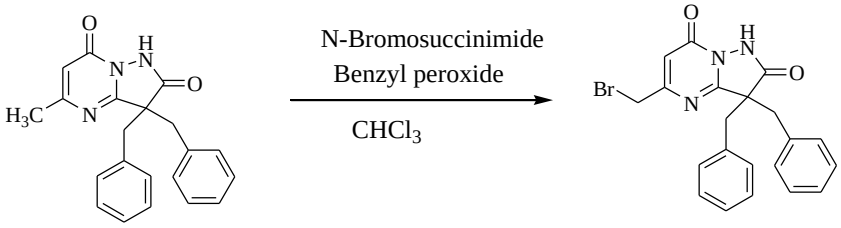

(1d)

In a 10 ml 2-neck RBF was kept on ice-bath wherein 3,3-dibenzyl-5-methylpyrazolo[1,5-*a*]pyrimidine-2,7(1*H*,3*H*)-dionewas dissolved in chloroform. To this *N*-bromosuccinimide (NBS) was added in portions. Once NBS was added, benzoyl peroxide was added and the reaction mixture was stirred at rt for 10 mins. Reaction was refluxed for 6 hours and the progress was monitored by TLC. Once the reaction was completed, excess chloroform was evaporated using rotary evaporator to obtain brownish residue. To the residue, crushed ice was added to obtain buff coloured solid, which was filtered with aid of vacuum. **Melting Point :** 176-179 °C**. IR**

(KBr, cm^{-1}): 3029, 2967, 2923, 2753, 1741, 1704, 1603, 1549, 1492 and 1385. **Mass**:[M] $^{+}$-424.61, [M+1] 425.61, [M+2] 426.66.

6.1.5 Synthesis of 5-((substitutedamino)methyl)-3,3-dibenzylpyrazolo[1,5-*a*]pyrimidine-2,7(1*H*,3*H*)-dione (28-34).

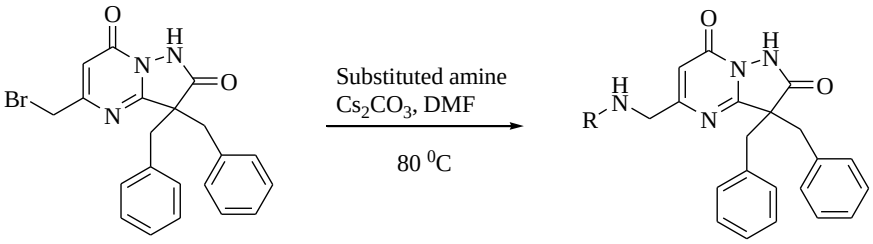

(1d) **(28-34)**

In a 25 ml 2-neck RBF substituted amine was dissolved in dry DMF and Cs_2CO_3 was added. After stirring at rt for 5-10 mins under the stream of nitrogen, 3, 3-dibenzyl-5-(bromomethyl)pyrazolo[1,5-*a*]pyrimidine-2,7(1*H*,3*H*)-dione was added and the reaction mixture was transferred on oil bath at 80 °C for 5-6 hrs. Progress of the reaction was monitored by TLC. After completion of reaction, crushed ice was added, extracted with chloroform and dried over Na_2SO_4. Solvent was evaporated using rotary evaporator and the sticky material so obtained was purified through column chromatography using petroleum ether and ethyl acetate (60%) as eluents to provide 5-((substitutedamino)methyl)-3,3-dibenzylpyrazolo[1,5-*a*]pyrimidine-2,7(1*H*,3*H*)-dione.

6.1.5.1 Synthesis of 5-((4-fluorobenzylamino)methyl)-3,3-dibenzylpyrazolo[1,5-*a*]pyrimidine-2,7(1*H*,3*H*)-dione (28)

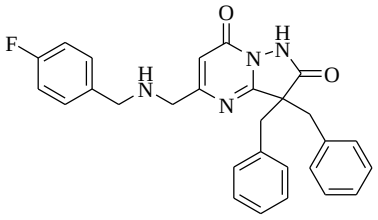

(28)

Compound (**28)** was synthesized using the method as mentioned in step 5 and by reacting 4-flourobenzyl amine with 3, 3-dibenzyl-5-(bromomethyl)pyrazolo[1,5-*a*]pyrimidine-2,7(1*H*,3*H*)-dione. Compound **28**was obtained as buff coloured solid.

Analysis:

Melting point: 173-177 °C**.**

TLC: R_f 0.45 (n-hexane:ethyl acetate; 8:12)

IR (KBr, cm^{-1}): 3030, 2921, 2853, 1637, 1568, 1511, 1382, 1226, 839 and 699.

^{1}H-NMR (δ): 7.789 (m, 3H), 7.443-7.210 (m, 4H), 7.047-6.993 (m, 8H), 5.709 (s, 1H), 3.875 (s, 2H), 3.068-3.027 (dd, 4H), 2.210 (s, 2H)

6.1.5.2 Synthesis of 5-((4-chlorobenzylamino)methyl)-3,3-dibenzylpyrazolo[1,5-*a*]pyrimidine-2,7(1*H*,3*H*)-dione (29)

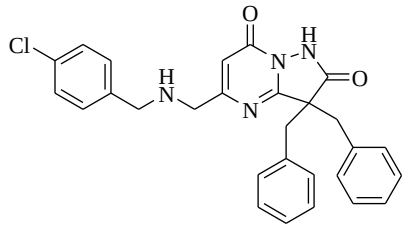

(29)

Compound **29** was synthesized using the method as mentioned in step 5 and by reacting 4-chlorobenzyl amine with 3, 3-dibenzyl-5-(bromomethyl)pyrazolo[1,5-*a*]pyrimidine-2,7(1*H*,3*H*)-dione to get the yellow coloured solid.

Structural Analysis:

Melting point: 182-185 °C**.**

TLC: R_f 0.5 (*n*-hexane:ethyl acetate; 8:12)

IR (KBr, cm^{-1}): 3026, 2917, 2849, 1614, 1571, 1492, 1202, 1092 and 698.

^{1}H-NMR (δ): 7.431(t, 4H), 7.070 (m, 6H), 7.026 (m, 5H), 3.866 (s, 2H), 3.173-3.051(dd, 4H), 2.459 (s, 2H).

6.1.5.3 Synthesis of 3,3-dibenzyl-5-((4-methylbenzylamino)methyl)- pyrazolo[1,5-*a*]pyrimidine-2,7(1*H*,3*H*)-dione (30)

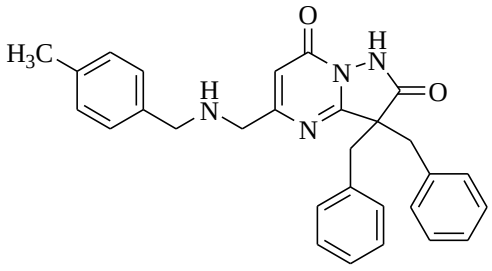

(**30)**

Compound **30** was synthesized using the method as mentioned in step 5 and by reacting 4-methylbenzyl amine with 3, 3-dibenzyl-5-(bromomethyl)pyrazolo[1,5-*a*]pyrimidine-2,7(1*H*,3*H*)-dione. Compound **30** was obtained as buff coloured solid.

Structural Analysis:

Melting point: 180-184 °C**.**

TLC: R_f 0. 47 (n-hexane:ethylacetate; 8:12)

IR (KBr, cm^{-1}): 3060, 3030, 2922, 2853, 1739, 1639, 1579, 1085 and 701.

^{1}H-NMR (δ): 7.135-7.092 (m, 8H), 7.003 (m, 7H), 3.539-3.402 (d, 2H), 3.221-3.065 (m, 2H), 2.340-2.270(m, 4H), 1.346-1.236(m, 4H).

6.1.5.4 Synthesis of 5-((2,4-dichlorobenzylamino)methyl)-3,3-dibenzylpyrazolo[1,5-*a*]pyrimidine-2,7(1*H*,3*H*)-dione (31)

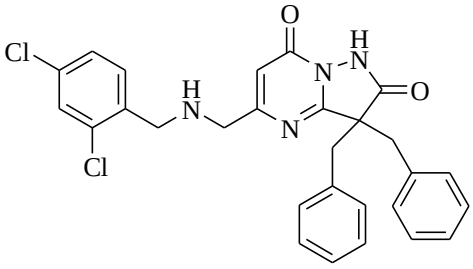

(31)

Compound **31** was synthesized using the method as mentioned in step 5 and by reacting 2,4-dichlorobenzyl amine with 3, 3-dibenzyl-5-(bromomethyl)pyrazolo[1,5-*a*]pyrimidine-2,7(1*H*,3*H*)-dione. Compound **31**was obtained as orange coloured solid.

Structural Analysis:

Melting point: 190-192 °C**.**

TLC: R_f 0. 54 *(n*-hexane:ethylacetate; 8:12)

IR (KBr, cm^{-1}): 3179, 3064, 3024, 2872, 1587, 1484, 1100 and 821.

Mass: 521.19 [M+2]

^{1}H-NMR (δ): 8.816 (s, 1H), 8.029-8.008 (d, 1H), 7.734(s, 1H), 7.663-7.340(m, 12H), 4.899 (s, 2H), 4.477-4.333(m, 4H), 4.285-4.173(d, 2H).

6.1.5.5 Synthesis of 3,3-dibenzyl-5-((pyridin-4-ylamino)methyl)pyrazolo[1,5-*a*]pyrimidine-2,7(1*H*,3*H*)-dione (32)

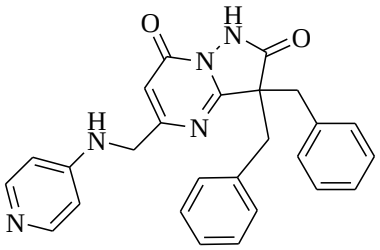

(32)

Compound **32** was synthesized using the method as mentioned in step 5 and by reacting 4-aminopyridine with 3, 3-dibenzyl-5-(bromomethyl)pyrazolo[1,5-*a*]pyrimidine-2,7(1*H*,3*H*)-dione. Compound **32** was obtained as brown coloured solid.

Structural Analysis:

Melting point: 178-181 °C**.**

TLC: R_f 0. (*n*-hexane:ethylacetate; 8:12)

IR (KBr, cm^{-1}): 3063, 3030, 2921, 1742, 1648, 1589, 1223, 1140 and 700.

Mass: 436.19 [M^+]

^{1}H-NMR (δ): 9.913 (s, 1H), 7.789 (m, 3H), 7.443-7.210 (m, 4H), 7.047-6.993 (m, 8H), 3.102-3.049 (dd, 6H).

6.1.5.6 Synthesis of 5-((4-methoxybenzylamino)methyl)-3,3-dibenzylpyrazolo[1,5-*a*]pyrimidine-2,7(1*H*,3*H*)-dione (33)

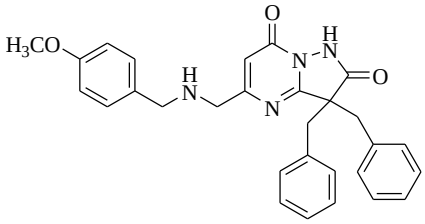

(33)

Compound (**33)** was synthesized using the same method as for compound **(28-32)** and by reacting 4-methoxybenzyl amine with 3, 3-dibenzyl-5-(bromomethyl)pyrazolo[1,5-*a*]pyrimidine-2,7(1*H*,3*H*)-dione. Compound **33** was obtained as yellowish colored solid.

Analysis:

Melting point: 183-185 °C**.**

TLC: R_f 0.44 (n-hexane:ethyl acetate; 8:12)

IR (KBr, cm^{-1}): 3030, 2921, 2853, 1637, 1568, 1511, 1382, 1226, 839 and 699.

6.1.5.7 Synthesis of 5-((2,4-dimethoxybenzylamino)methyl)-3,3-dibenzylpyrazolo[1,5-*a*]pyrimidine-2,7(1*H*,3*H*)-dione (34)

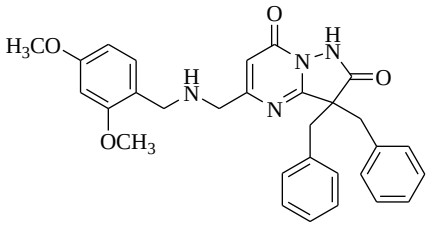

(34)

Compound (**34)** was synthesized using the same method as for compound **(28-32)** and by reacting 3, 4-dimethoxybenzyl amine with 3, 3-dibenzyl-5-(bromomethyl)pyrazolo[1,5-*a*]pyrimidine-2,7(1*H*,3*H*)-dione. Compound **34** was obtained as brown colored solid.

Analysis:

Melting point: 190-193 °C**.**

TLC: R_f 0.58 (*n*-hexane:ethyl acetate; 8:12)

IR (KBr, cm^{-1}): 3036, 2929, 2853, 1631, 1588, 1521, 1282, 1226, 859 and 689.

6.2 Synthesis and characterization of di-(4-methylbenzyl)substituted derivatives

6.2.1 Synthesis of methyl- 2, 2-(4-methylbenzyl)-2-cyano-ethanoate (35)

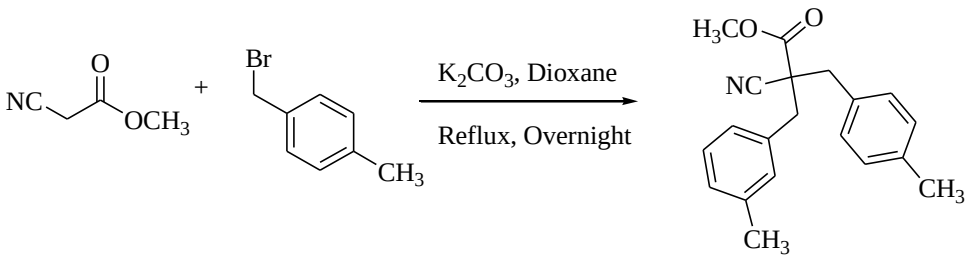

(**35**)

To a solution of methyl cyanoacetate and potassium carbonate in dioxane stirred under nitrogen atmosphere at 0° C was added a solution of 4-methylbenzyl bromide in dioxane. The reaction mixture was stirred at 80 °C for overnight. The reaction mixture was diluted with ice cold water and extracted with ethyl acetate (thrice). The combined organic layer was washed with water and brine, dried over anhydrous sodium sulphate and concentrated to dryness in vacuum to obtain colourless liquid product. This product was directly taken for next step without further purification. Its boiling point was found to be 89-91 °C. **IR** (KBr cm^{-1}): 3063, 3032, 2956, 2252, 1748, 1445, 1235, 620.

6.2.2 Synthesis of 4,4-di(4-methylbenzyl)-5-iminopyrazolidin-3-one (36).

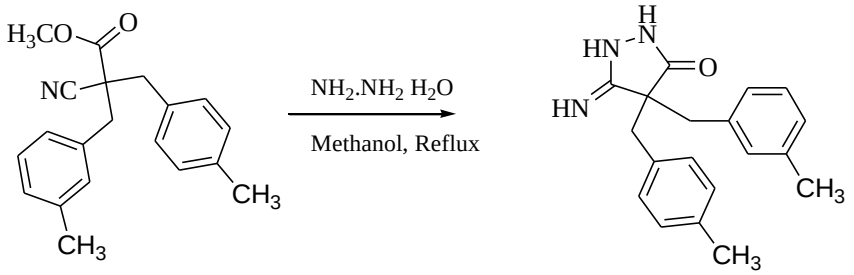

(35) **(36)**

To a solution of methyl- 2, 2-(4-methylbenzyl)-2-cyano-ethanoate in methanol stirred under nitrogen environment at room temperature, hydrazine hydrate (99 %) was added drop wise. The reaction mixture was refluxed at 80 °C overnight. After cooling, the reaction mixture was evaporated to dryness in vacuum. The residue was recrystallized using chloroform to provide white coloured solid product having a melting point greater than 250 °C. **IR** (KBr, cm^{-1}):3430, 3066, 2920, 2861, 1686, 1632 and 1448.. **Mass**: 308 [M+1].

Scheme for the synthesis of mono-substituted (XII) prototype is being carried out using scheme 02.

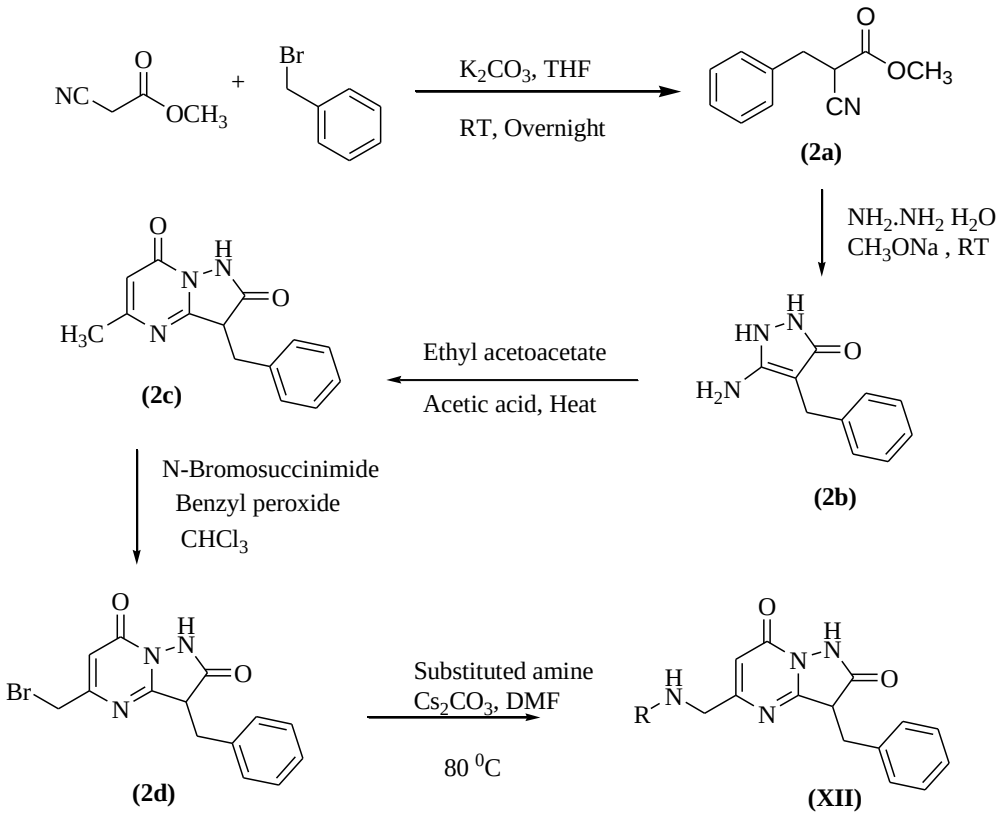

Scheme 2: Synthetic scheme of mono-substituted derivatives (XII)

6.3. Synthesis and characterization of mono-substituted derivatives.

6.3.1 Synthesis of methyl-2-cyano-3-phenylpropanoate (2a).

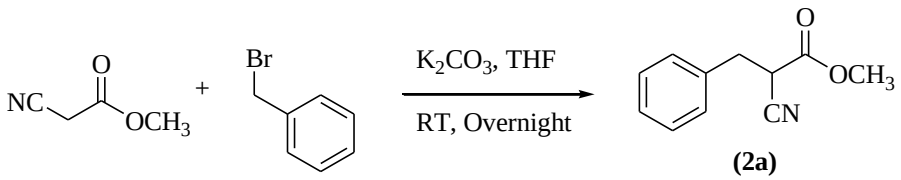

To a solution of methyl cyanoacetate and potassium carbonate in THF stirred under nitrogen atmosphere at 0° C, benzyl bromide was added. The reaction mixture was then stirred at room temperature for overnight. The reaction mixture was diluted with triethylamine and extracted with ethyl acetate (thrice). The combined organic layer was washed with water and brine, dried over anhydrous sodium sulphate and concentrated to dryness in vacuum to obtain clear liquid product. This product was directly taken for next step without further purification. Its boiling point was observed to be 156-158°C. **IR** (KBr cm^{-1}): 3063, 3032, 2956, 2252, 1748, 1445, 1235.

6.3.2: Synthesis of 5-amino-4-benzyl-1,2-dihydropyrazol-3-one (2b).

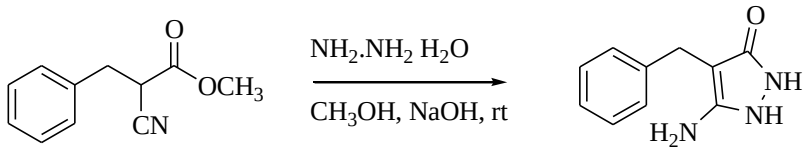

(2b)

To a solution of methyl-2-cyano-3-phenylpropanoate in methanol stirred under nitrogen environment at room temperature, hydrazine hydrate (99 %) was added drop wise. The reaction mixture was stirred at room temperature for 15 minutes. Sodium hydroxide pellets were added to the reaction and the mixture was allowed to stir for further 3 hours. The mixture was diluted with water, which was then filtered to obtain white coloured solid. Melting point was observed to be 178-180 °C. **IR** (KBr, cm^{-1}):3169, 3067, 2925, 2802, 1676, 1608, 1494 and 1002. **^{1}H-NMR**: δ 11.36 (s, 1H), 9.56 (s, 1H), 7.26-7.19 (m, 5H), 7.13 (m, 1H) and 3.58 (s, 2H).

6.3.3 Synthesis of 3-benzyl-5-methylpyrazolo[1,5-*a*]pyrimidine-2,7(1*H*,3*H*)-dione (2c)

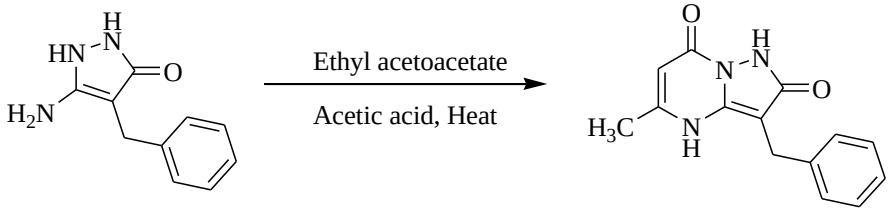

(**2b**) (**2c**)

To a solution of 5-amino-4-benzyl-1,2-dihydropyrazol-3-one in acetic acid, ethyl acetoacetate was added drop wise and stirred at room temperature for 10 minutes. Then, the reaction mixture was heated at 100 °C overnight. The reaction mixture was then diluted with ice cold water to obtain white coloured solid product. **Melting Point :** 178-180 °C**. IR** (KBr, cm^{-1}): 3060, 3030, 2750, 1739, 1638, 1549, 1451, 1267. Mass: 254 (M-1), 256 (M+1).

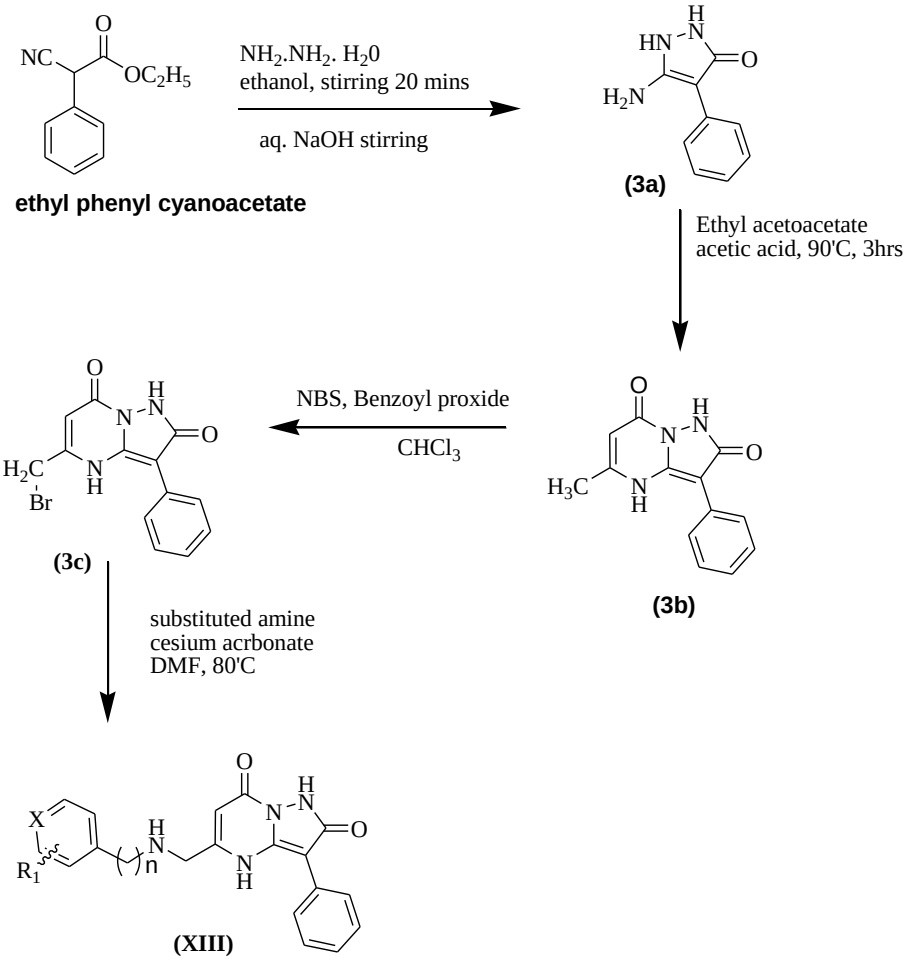

Scheme 3: Synthetic scheme for prototype XIII.

6.4 Synthesis and Characterization of phenyl substituted derivatives

6.4.1: Synthesis of 5-amino-1,2-dihydro-4-phenylpyrazol-3-one (3a).

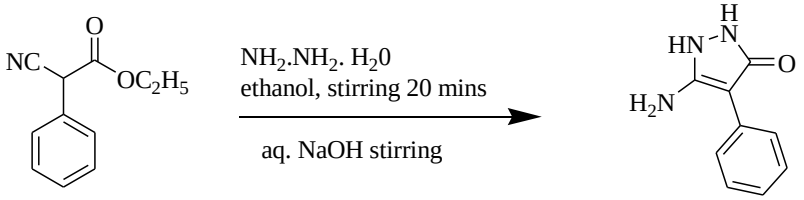

(3a)

In a single neck 25 ml RBF, Ethyl phenylcynaoacetate was added to ethanol. To this solution, hydrazine hydrate 90% was added drop-wise and the reaction mixture was stirred vigoursly for 5 mins. Aqueous NaOH solution was added to the reaction and further stirred for 15 mins. The completion of reaction mixture was monitored by TLC. After completion of reaction, dilute HCl was added to the reaction mixture to yield white solid product which was filtered under vacuum.

Melting point of the product was found to be 250-252 °C. **IR** (KBr, cm^{-1}): 3303, 3255, 3151, 1646, 1620, 1433, 1314. **Mass**: 176 [M+1].

6.4.2: Synthesis of 5-methyl-3-phenylpyrazolo[1,5-*a*]pyrimidine-2,7(1*H*,4*H*)-dione (3b).

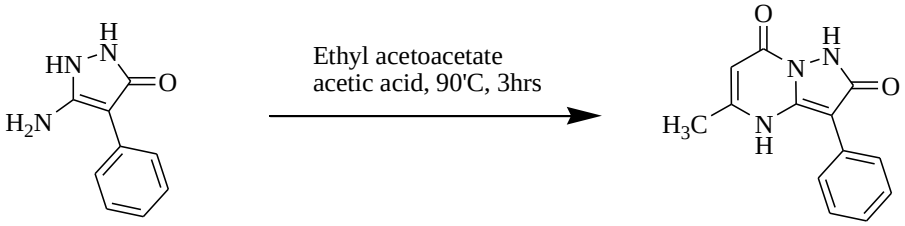

(3a) **(3b)**

To a solution of 5-amino-1,2-dihydro-4-phenylpyrazol-3-one in acetic acid, ethyl acetoacetate was added drop wise and stirred at room temperature for 10 minutes. Then, the reaction mixture was heated at 90 °C overnight. The reaction mixture was then diluted with ice cold water to obtain white coloured solid product. **Melting Point :** >250 °C**. IR** (KBr, cm^{-1}):3066, 3022,2948, 1688, 1645, 1606, 1500, 1442.. **Mass**: 242 [M+1].

6.4.3: Synthesis of 5-(bromomethyl)-3-phenylpyrazolo[1,5-*a*]pyrimidine-2,7(1*H*,4*H*)-dione (3c).

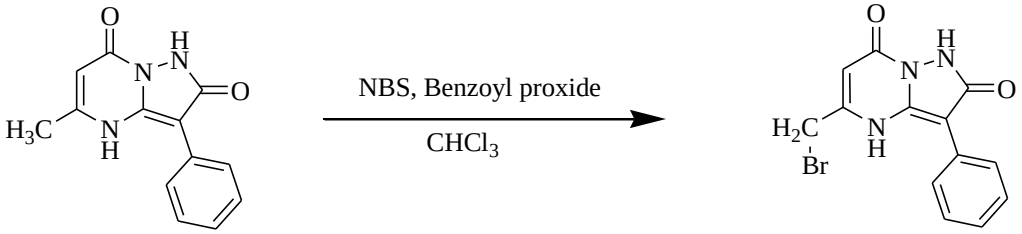

(3b) **(3c)**

In a 10 ml 2-neck RBF was kept on ice-bath wherein 5-methyl-3-phenylpyrazolo[1,5-*a*]pyrimidine-2,7(1*H*,4*H*)-dione was dissolved in chloroform. To this *N*-bromosuccinimide (NBS) was added in portions. Once NBS was added, benzoyl peroxide was added and the reaction mixture was stirred at rt for 10 mins. Reaction was refluxed for 6 hours and the progress was monitored by TLC. Once the reaction was completed, excess chloroform was evaporated using rotary evaporator to obtain brownish residue. To the residue, crushed ice was added to obtain buff coloured solid, which was filtered with aid of vacuum. **Melting Point :** >250 °C**. IR** (KBr, cm^{-1}): 3056, 2962, 1634, 1578, 1260, 694.

The above synthesized derivatives are pyrazolo-pyrimidine derivatives which has been designed based on the results of computational studies such as pharmacophore modelling, virtual screening etc.

Recently there have been many research work going on chalcone derivatives as anti-tubercular agents [25-27]. Also, some researchers have been working on chalcone derivatives as DprE1 inhibitors [28]. The authors Kumar *et al.* synthesized and performed docking studies for chalcone derivatives, wherein they showed that these chalcone derivatives are binding potently to the DprE1 enzyme. From the literature it was noted that many five membered heterocycles such as triazole, thiazoles etc were exhibiting excellent DprE1 inhibition [20-22].

We have already synthesized some pyrazole derivatives. Therefore, it was planned to incorporate chalcone moiety fused with pyrazole using hybrid approach. Structure **IV** represents the prototype of hybrid approach molecule.

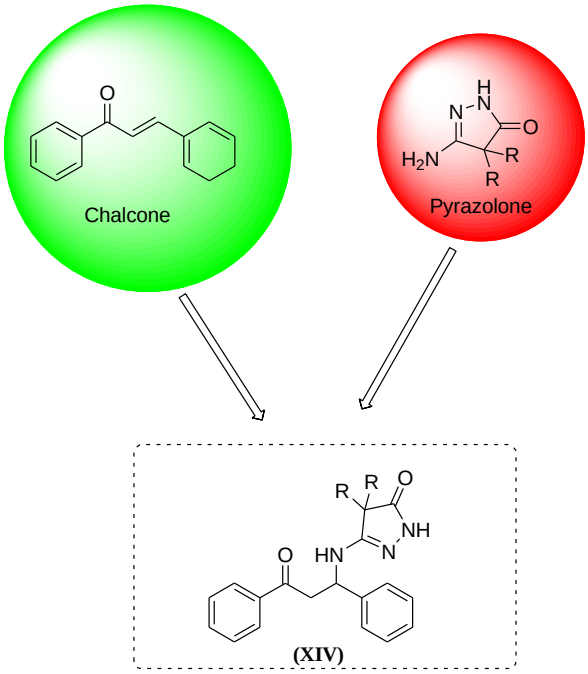

Figure 13: Designing of hybrid prototype XIV.

6.5 Scheme for synthesis of chalcone derivatives

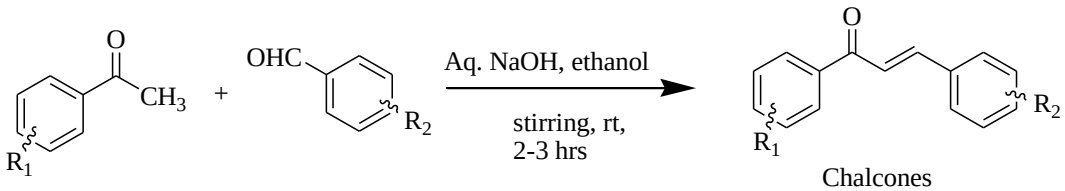

R_1= H, 4-Cl

R_2= 2-NO_2, 3-NO_2, 4-NO_2, 3-Br, 4-Br, 3-F, 4-F, 4-CH_3

To a RBF containing ethanol, aqueous NaOH solution was added on ice bath with continuous stirring. To this acetophenone was added and allowed to stir for 5 mins. The reaction mixture was brought to rt and substituted benzaldehyde was added with continuous stirring. The reaction mixture was stirred vigouorsly at rt for 2-3 hours and reaction was monitored by TLC. Upon completion, crushed was added to the reaction mixture to obtain solid chalcones. These were taken for further reaction without purification.

Table 5: Results for synthesized chalcones

R_1	**R_2**	**R_f (Hexane: ethyl acetate)**	**Melting point (°C) (Reported value) [25-28]**	**% Yield**
H	2-NO_2	0.2	104-109	48
H	3-NO_2	0.16	140-141 (145-146)	77
4-Cl		0.43	115-120	110
H	4-NO_2	0.36	160-164 (160-166)	67
4-Cl		0.6	140-145	114
H	3-F	0.5	55-60	97
4-Cl		0.64	95-100	120
H	4-F	0.5	94-96	98
H	3-Br	0.5	85-90 (83-86)	159
4-Cl		0.64	112-116	89
H	4-Br	0.5	120-124 (119-120)	155
4-Cl		0.72	135-140	97
H	4-CH_3	0.5	104-110	99

4-Cl		0.72	122-127	110

6.6 Synthesis of hybrid prototype (IV)

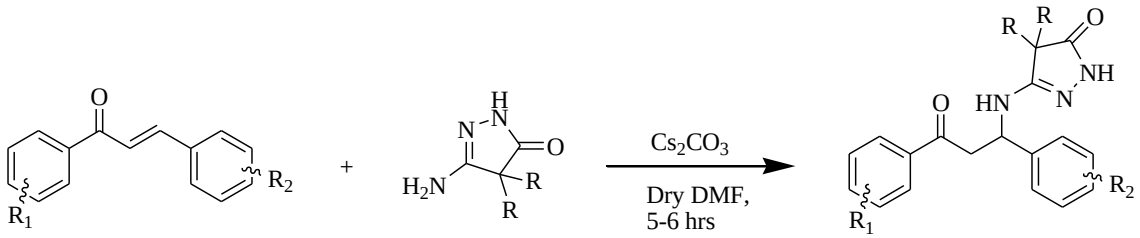

(IV)

In a two-neck 25-ml RBF, pyrazolone was dissolved in a mixture of cesium carbonate in dry DMF. This mixture was allowed to stir at rt under a stream of nitrogen. To this mixture, chalcone was added portion-wise. The reaction mixture was heated at 80 °C for 5-6 hours. Reaction was monitored by TLC. Upon completion, crushed ice was added to the reaction mixture. The product was filtered under vacuum to obtain orange colored solid compound. The product was purified by column chromatography using petroleum ether and ethyl acetate (20%).

6.6.1 Synthesis of 3-(1-(4-chlorophenyl)-3-oxo-3-phenylpropylamino)-4,4-dibenzyl-1*H*-pyrazol-5(4*H*)-one (37)

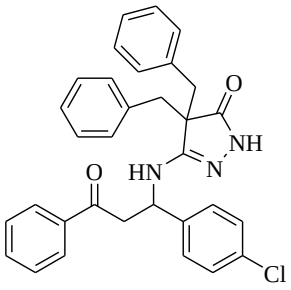

(37)

Compound (**37)** was synthesized using the same method as for compound IV and by reacting 4-chlorochalcone with 4,4-dibenzyl-5-iminopyrazolidin-3-one. Compoundwas obtained as orange colored solid.

Analysis:

Melting point: 218-220 °C**.**

TLC: R_f 0.62 (n-hexane:ethyl acetate; 10:10)

IR (KBr, cm^{-1}): 3057, 2984, 2934, 1711, 1657, 1511

Mass: 522 (M^+), 523 (M+1), 525

7. Computational studies

Docking studies were performed for the synthesized compounds. Autodock of MGL tools 1.5.6 were used for protein preparation, ligand preparation and grid generation and autodock4 software for docking. Docking pair of protein and ligand generated from autodock vina was saved in pdbqt format and were visualized in Discovery studio. In Discovery studio the molecular interactions in the form of hydrogen bonds between protein and ligands were characterized. The summary of docking studies is summarized in the **Table 6**. Ligand-enzyme interaction for compound is shown in **Figure 14**. Docking studies of compound have shown two strong hydrogen bonding interactions. The H-bond can be seen between fluoro of compound 1 and amino acid residue Arg A.58 and Thr. 118. Such hydrogen bonding interactions serves as 'anchor' guiding the 3D orientation of the ligand in the active site. The phenyl ring present in the compound was interacting with various amino acid residue via pi-sigma and pi-alkyl interaction.

Table 6: Binding affinity of the docked compounds (PDB id: 4p8n)

Compound ID	**Binding affinity (kcal/mol)**
28	-10.5
29	-9.8
30	-9.9
31	-9.6
32	-9.7
33	-9.9
34	-9.8
QN-118 (standard)	-9.9

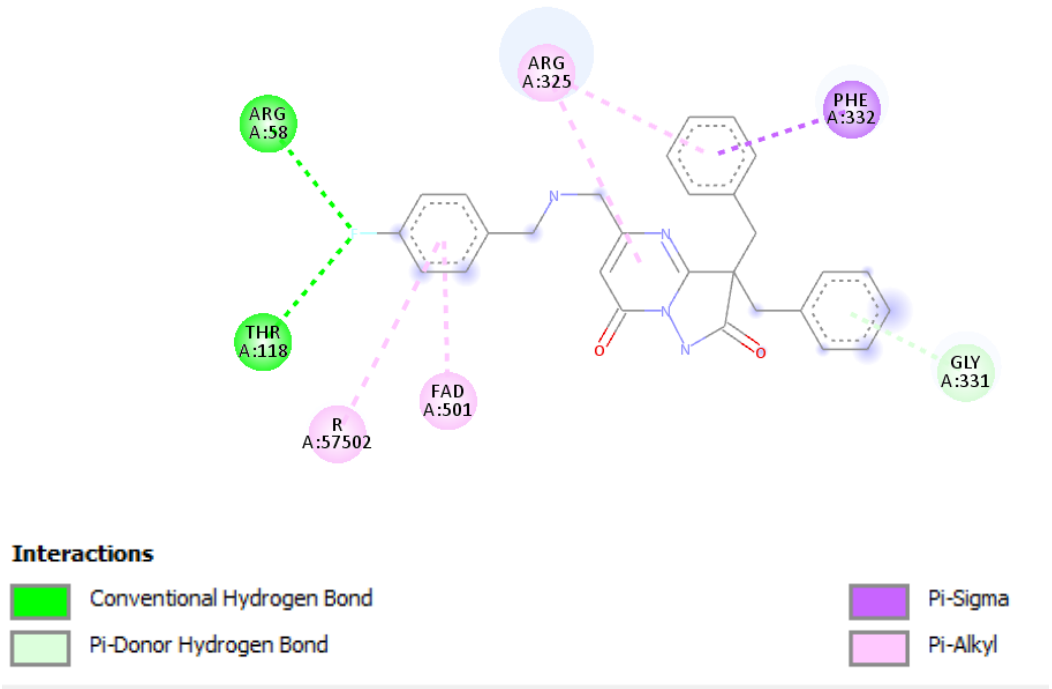

Figure 14: Ligand enzyme interaction of compound 28.

Furthermore, *in-silico* ADME properties were predicted using SwissADME. The predicted properties are summarized in **Table 7.**

Table 7: *In-silico* ADME prediction

Comp ID	Molecular weight	Topological polar surface area (Å)	GI absorption	Water solubility	Lipo-philicity (MLOGP)	Cytochrome P450 1A2 inhibitor	Lipinski rule violation
28	468	76.02	High	-5	3.85	No	0
29	484	76.02	High	-5.43	3.94	No	0
30	464	76.02	High	-5.14	3.68	No	0
31	519	76.02	High	-6.03	4.41	No	2
32	437	88.91	High	-4.56	2.55	No	0

8. BIOLOGICAL ACTIVITY

The synthesized compounds will be sent for biological evaluation for their anti-tubercular activity. The screening is to be done at CSIR laboratory Lucknow where the samples will be

screened using Microplate Alamar Blue Assay (MABA) against Mycobacterial pathogens namely *M Chelone, M. abscessus, M. fortuium, M. tuberculosis*. The potent compounds will then be subjected to Mycobacteria growth indicator tube (MGIT) assay.

PUBLICATIONS (Related to present work)

1. Mange Ram Yadav, Prashant R. Murumkar, **Monica Chauhan**, Rahul B. Ghuge, Rahul R. Barot. Exploring decaprenylphosphoryl-β-*D*-ribose 2'-epimerase 1(DprE1)- A druggable target for designing of DprE1 inhibitors as anti-tubercular drugs (Communicated)

References:

1. https://www.who.int/health-topics/tuberculosis#tab=tab_1
2. Gawad, J. *Indian J. Tuberculosis***2018**, *65*, 15-22.
3. Vasava, M. S. *Indian J. Tuberculosis***2017**, *64*, 252-275.
4. Mikusova, K. *Drug Discov. Today***2017**, *22*, 534-545.
5. Chikhale, R. V. *J. Med. Chem.***2018**, *61*, 8563-8593.
6. Moreno E., *et. al.*, Eur. J. Med. Chem., **2010**, 45, 4418-4426.
7. Patel SR., *et. al.*, Eur. J. Med. Chem., **2015**, 93, 511-522.
8. MajewskiMW.,*et. al.*, Bioorg. Med. Chem. Lett., **2016**, 26, 2068-2071.
9. Klein L,.*et.al.*,Bioorg. Med. Chem. Lett., **2014**, 24, 268-270.
10. Ivani p., *et. al.*, J. Chem. Inf. Model., 2013, 53, 2390-2401.
11. Degiacomi G, ApplSci, **2020** 10(2):623.
12. Filomena M., *et.al*., Eur. J. Med. Chem., 2014, 81, 119-138.
13. Stanley SA.,*et. al.*, Chem. Biol., **2012**, 7, 1377-1384.
14. Yashang L., *et. al.*, Biochem. Pharmacol.,**2013**, 86, 222-230.
15. Pathak AK., *et.al.*,Bioorg. Med. Chem. Lett., **2002**, 12, 2749-2752.
16. Shirude P., *et. al.*, J. Med. Chem., **2014,** 57, 5728−5737.
17. Tiwari R., *et. al.*, Med. Chem. Lett., 2015, 6, 128-133.

18. Garner, A. L., *et.al.Mol. Microbiol.***2014**,*93*, 682-697.

19. Susan ek.,*et.al. Tuberculosis. **2014**, 94, 271-276.*

20. Rammohan, J., *et.al., Nucleic Acids Res.* **2016**, *44*, 7304-7313

21. Kgothatso EM., *et.al. Cell biochemBiophys 2016, 74, 473-481*.

22. Neres J, Sci Trans Med 4(150), **2012**:150ra121-150ra121.

23. Batt SM, Proc Natl AcadSci ,**2012**, 109(28):11354-11359.

24. Hariguchi N, AntimicrobAgents Chemother, **2020** 64(6):e02020-19. doi: 10.1128/AAC.02020-19.

25. Gomes MN. *et. al.* Eur J Med Chem, **2017**, doi: 10.1016/j.ejmech.2017.05.026.

26. Lin MY., *et.al.* Bioorg Med Chem, **2002**, 10, 2795, 2802.

27. Castano LF., *et al.* Eur J Med Chem, **2019**, 176, 50-60.

28. Kumar G. *et. al.* Arch Pharm, **2020**, DOI: 10.1002/ardp.202000077.

****